2018

Statistically Quantifying the Efficacy of MCS Predictive Parameters in Pinpointing the Location of Initiation of an MCS in the Great Plains Region

Samuel Luthi
Iowa State University

Statistically Quantifying the Efficacy of MCS Predictive Parameters in Pinpointing the Location of Initiation of an MCS in the Great Plains Region

Samuel Luthi

Department of Geological and Atmospheric Sciences, Iowa State University, Ames, Iowa

Dr. William Gallus, Jr. – Mentor

Department of Geological and Atmospheric Sciences, Iowa State University, Ames, Iowa

ABSTRACT

Accurate forecasting of MCSs is an incredibly important aspect of operational meteorology, given their propensity to cause damage to property and loss of life. Studies regarding MCSs vary greatly, but few examine parameter efficacy in predicting the initiation point of a given warm-season MCS in the Great Plains. This study examined the efficacy of five parameters: 700mb warm-air advection (WAA), 850mb mixing ratio, 850mb equivalent potential temperature advection (θ_E), surface frontogenesis, and 850mb convergence. 29 cases were analyzed in total. None of the analyzed parameters proved to stand out in accurately predicting an MCS initiation point in terms of distance from the parameter maximum to the MCS centroid, the direction of the parameter maximum with respect to the MCS centroid, and the latitude and longitude differences between the parameter maximum and centroid of the MCS. One parameter did have potentially useful results. 700mb WAA was found to be to the northeast in 50% of the cases, indicating a potential correlation. In general, there does not appear to be a parameter that works substantially better than others that forecasters should use above others when forecasting MCS initiation location.

---

1. Introduction

Since first defined in 1980 by Maddox, the Mesoscale Convective Complex (from henceforth, an MCC) remains a particularly unique phenomenon for the Great Plains region of the United States and a phenomenon of great interest to researchers. These types of thunderstorm complexes often account for the large majority of warm season rainfall in the Great Plains region. This copious amount of rainfall has major benefits when it comes to the agrarian nature of the Great Plains region, and is often seen as advantageous, as opposed to being detrimental. However, MCCs often have devastating implications for the regions that they affect. The aforementioned torrential rain, while beneficial for sustainable agriculture, can also cause extreme flash flooding events in a region. In addition, hail and damaging winds are also possible accompaniments to these systems. When

these damaging winds organize themselves in the form of intense downdrafts, a severe threat to aviation is present in the vicinity of the system.

Due to the threats contained within these systems, it is imperative for operational forecasters to better understand the efficacies of certain predictive parameters in pinpointing the initiation location of any given MCC in the Great Plains region during the warm season. In total, the main focus of this research will answer the question: which of the MCC predictive parameters (theta-e advection, mid-level warm air advection, maximum convergence synchronous with the nose of the nocturnal low-level jet, and stationary front positioning) most accurately forecasts the initiation location of an MCC in the Great Plains region during the warm season?

2. Background

A mesoscale convective complex (MCC) was first defined in 1980 by Maddox from NOAA's Office of Weather Research. The definition of an MCC is routinely based on the physical characteristics of the system that can be observed on infrared satellite imagery (Maddox 1980). Such characteristics include the cloud shield of the system exceeding 100,000 km^2 and having a temperature less than or equal to -32° Celsius and the region of coldest cloud tops must exceed 50,000 km^2, having temperatures less than or equal to -52° Celsius (Maddox 1980). The eccentricity of the minor axis to the major axis must be greater than or equal to 0.7 at the time the system is at its largest and most mature stage (Maddox 1980). In addition to these spatial characteristics, one temporal characteristic is defined by Maddox: the system must perpetuate its spatial dimensions for a time period of at least 6 hours (Maddox 1980).

Along with the provision of defining characteristics of MCCs, Maddox also demonstrated a multitude of other factors that separate MCCs from other types of thunderstorm phenomena. Most notably, Maddox identified that MCCs are convectively-driven systems of thunderstorms, unlike systems such as squall lines, which typically arise from synoptic features such as frontal boundaries (Maddox 1980).

Continuing his work on MCCs, Maddox examined a particular MCC case in the Mississippi Valley area during the beginning of the warm season. Through this work, Maddox identified that such convectively-driven systems have the ability to strongly alter the upper-level flow and environmental conditions in the region they impact, such as causing the flow to strongly diverge at the 20kPa level during a 6-hour period (Maddox 1981). The work done by Maddox set a foundation for other meteorologists to build off when it comes to MCC research.

Cotton et al. in 1989 worked to further understand MCC structure and presented a dynamically-based definition of an MCC. The evolution of wind, thermodynamic, divergence, vertical velocity, and vorticity fields were studied provide such a definition, and the resulting analyses were used to generate an expanded conceptual model of an MCC. Fields analyzed during the Cotton et al. study that are notable concerning this study include the 850mb mixing ratio, 850mb

convergence, 700mb temperature advection, and 850mb equivalent potential temperature advection. The study found that convergence, vertical motion, and heating in low levels are most characteristic of the early life stages of an MCC, shifting to upper levels as the MCC matures.

Studies done on MCCs tend to focus on identifying and understanding the methods by which MCCs impact society most directly. Much work has been done that looks at extreme precipitation producing MCCs and MCSs, based on the detrimental effect such precipitation has on the population over a relatively small area. Focusing on the MCSs that impacted the Nashville, TN area from May 1st to May 2nd of 2010, Moore, Neiman, Ralph, and Barthold identified numerous environmental characteristics that increased the potency of the MCSs, ultimately having a greater effect on the Nashville area. One such characteristic noted was the role that an Atmospheric River (AR) played in intensifying the precipitation of the systems. This intensification arises from the combination of a southerly low-level jet (LLJ) advecting in large quantities of moist, tropical air, along with large CAPE values which both often result in deep moist convection (Moore et al. 2012). In the case of Nashville, this unstable airmass remained relatively stagnant over the region, causing the resulting MCS to remain over the region and cause heavy precipitation that resulted in flash flooding events over the two-day time period.

Other research performed in the area of extreme precipitation producing MCSs and MCCs has yielded more information about the environmental characteristics that cause such scenarios. Schumacher and Johnson identified two patterns of organization of such extreme systems. One such pattern, "training line, adjoining stratiform," is organized in an east-west fashion and often moves in the line-parallel direction, exposing the same regions to multiple rounds of heavy rainfall (Schumacher and Johnson 2005). Often these systems are accompanied by environmental features such as a stationary front or other boundary to the south of the system, as well as the mid-level shear and cell motion being aligned parallel to the boundary present (Schumacher and Johnson 2005). The other pattern identified was referred to as a back-building (BB) system. These systems typically develop and depend on environments that exhibit stronger mesoscale features, such as storm-generated outflow boundaries and cold pools, rather than synoptic boundaries that the previous classification depends on (Schumacher and Johnson 2005).

The low-level jet (LLJ) has often been identified as a contributing factor to the formation of MCSs. In a two-part paper by Squitieri and Gallus in 2016, the relationship between LLJ forecast accuracy and MCS precipitation forecast skill was examined in-depth. Research demonstrated that LLJ forecast accuracy had a strong correlation with precipitation forecast skill when the MCS in question originated in a strongly forced synoptic background with cyclonic flow (Squitieri and Gallus 2016). However, in weakly forced, anticyclonic flow environments, it was found that LLJ forecast accuracy and precipitation forecast skill did not have any significant correlations,

indicating that factors unrelated to the LLJ may have more significant effects than the LLJ itself (Squitieri and Gallus 2016).

Part two of Squitieri and Gallus (2016) focused on a comparison of forecasted LLJ events with MCSs in both strongly and weakly forced synoptic environments. In convection-allowing WRF forecast simulations, it was found that MCSs tended to initiate north and east of observations where parameters such as moisture, MUCAPE, and MUCIN fields were forecasted accurately (Squitieri and Gallus 2016).

From this, it can be seen that much of the MCS and MCC research focuses more on extreme cases, or focusing specifically on a single parameter's accuracy with respect to the precipitation produced by a given MCS. Research involving rule-of-thumb forecast parameter accuracy with respect to initiation location is sparse at best. This research intends to address the current gap in MCS forecast parameter accuracy research by analyzing whether prior study findings, such as useful forecasting parameters, apply well to the overall category of MCSs, and not just MCCs. Knowing which parameters most accurately forecast initiation location, or even knowing the biases that certain parameters tend toward, has the potential to be indispensable for operational forecasters.

3. Data and Methods

a. Case Selection

A set of 29 cases taken from Squitieri & Gallus 2016 were selected in accordance with the following criteria:

1. Case must contain a nocturnal MCS in the defined domain (Fig. 1).
2. Case must have the presence of the Great Plains nocturnal low-level jet in Rapid Update Cycle (RUC)/Rapid Refresh (RAP) analyses.
3. Case must have occurred during the warm season (May through August).

Cases were downloaded as 13km RUC analyses from the time period of 2009 to 2011. After 2011 13km RAP analyses were used due to the replacement of the RUC model. RUC and RAP data was downloaded from the National Centers for Environmental Information (NCEI) THREDDS catalog. Composite reflectivity RADAR data was

obtained from the National Center for Atmospheric Research (NCAR) Research Data Archive in the form of GridRad data. Parameters were recorded 3 hours before the time of the MCS initiation.

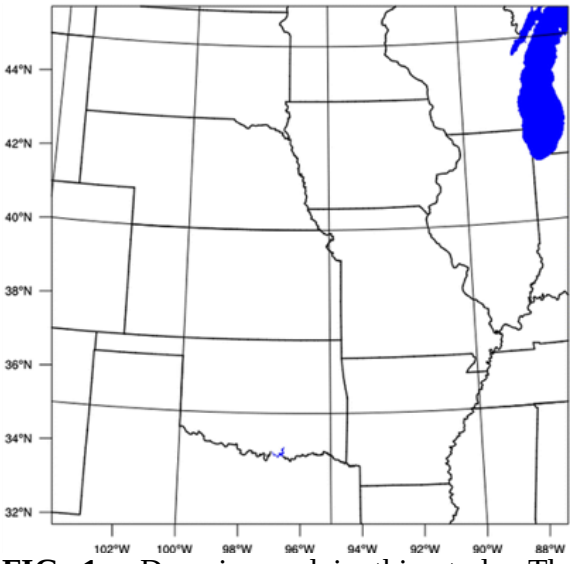

FIG. 1 - Domain used in this study. The domain is coincident with that of Squitieri & Gallus 2016.

b. Parameters

A total of five separate parameters were calculated:

1. 700mb Warm Air Advection (WAA)
2. 850mb Mixing Ratio
3. 850mb Equiv. Pot. Temperature Advection (Θ_e)
4. Surface Frontogenesis
5. 850mb Convergence

700mb WAA, 850mb mixing ratio, 850mb equivalent potential temperature (henceforth, Θ_e), and 850mb wind speed were all chosen to coincide with rule-of-thumb parameters looked at by Cotton et al. in 1989. Surface frontogenesis was added to observe the effects of frontal lifting of MCS initiation location in a quantitative manner, as opposed to qualitatively analyzing surface maps which would potentially increase error within the study.

c. Calculation of Parameters

Warm air advection was calculated with an intrinsic Python package function, following a multiplication of a temperature array with arrays containing data representing wind speed and direction at a given level.

850mb mixing ratio was derived from the relative humidity at 850mb. The formula used to calculate the mixing ratio was adapted from Wallace and Hobbs in 1977:

$$(1)\ w = (RH)(w_s)$$

Where 'w' refers to the mixing ratio, 'RH' refers to the relative humidity, and 'w_s' refers to the saturation mixing ratio. All quantities in this equation are unitless, but the mixing ratio was defined in units of gram per gram.

Equivalent potential temperature advection (Θ_e) was calculated using a formula found in a 1980 Bolton article specifically regarding the numerical computation of equivalent potential temperature. The formula, according to Davies and Jones in 2009, is the most accurate formulation available that is non-iterative. The calculation used comprises multiple steps outlined below:

1. Calculate the Lifted Condensation Level (LCL) temperature:

$$(2)\quad T_L = \frac{1}{\frac{1}{T_D - 56} + \frac{\ln(T_K/T_D)}{800}} + 56$$

2. Calculate the potential temperature at the LCL:

$$(3)\quad \theta_{DL} = T_K\left(\frac{1000}{p - e}\right)^k \left(\frac{T_K}{T_L}\right)^{0.28r}$$

3. Utilizing the two values above, Θ_e is calculated as such:

$$(4)\quad \theta_E = \theta_{DL}\exp[\left(\frac{3036}{T_L} - 1.78\right) * r(1 + 0.448r)$$

Where Θ_E refers to the equivalent potential temperature, T_K refers to the absolute temperature (given by the equation: $T_K = T + 273.15$), T_D refers to the dewpoint temperature, T_L refers to the LCL temperature, and Θ_{DL} refers to the potential temperature at the LCL level. Other constants in the equations can be referred to the Bolton 1980. Θ_E advection was calculated in a similar manner to warm air advection.

Surface frontogenesis (specifically the two-dimensional kinematic frontogenesis of a temperature field) was calculated using the formula outlined by Bluestein in 1993, and is a form of Petterssen frontogenesis:

$$(5)\quad F = \frac{1}{2}|\nabla\theta|[Dcos(2\beta) - \delta]$$

Where F refers to the two-dimensional kinematic frontogenesis, Θ refers to the potential temperature, D refers to the total deformation, β refers to the angle between the axis of dilatation and the isentropes, and δ refers to the divergence.

850mb convergence was calculated from the 'u' and 'v' components of the wind, where the 'u' and 'v' refer to the wind components in the east-west and north-south direction respectively. The formula for divergence is outlined below:

$$(6)\quad \delta = \frac{du}{dx} + \frac{dv}{dy}$$

d. Parameter Analysis

Parameters were plotted on a map of the domain, and the maximum value of a given parameter was marked with a black dot (Fig. 2). Both the longitude and latitude of the maximum parameter value were recorded. The centroid of the composite reflectivity was also plotted on a map of the domain, with the centroid marked as well. The longitude and latitude of this centroid were recorded. The distance between the coordinates of the maximum parameter value and the centroid of composite reflectivity was recorded for all parameters. These distances were compared to each other, with box and whisker plots being used to provide a visual representation of each parameter's efficacy in predicting the initiation point for an MCS in a given case. Additionally, latitudinal and longitudinal differences were recorded for each parameter. These differences were calculated by finding the latitudinal or longitudinal difference between the parameter maximum and the centroid of the MCS.

4. Results and Analysis

a. 700mb Warm Air Advection

Warm air advection at the 700mb level displayed a wide range of distances from its maximum intensity point to the centroid of the relevant MCS. On average, the maximum point of 700mb WAA was located approximately 617 kilometers away from the centroid of the MCS, with maximum distances of 1494km and 158km respectively.

When analyzing the direction of the WAA with respect to the centroid of the MCS, it was found that the maximum point of WAA was located to the northeast (out of the eight cardinal and intermediate directions) of the

MCS centroid in 50% of the cases. Additionally, the maximum point of WAA was found to the east, southwest, and west of the MCS centroid in 21%, 18%, and 11% of the cases.

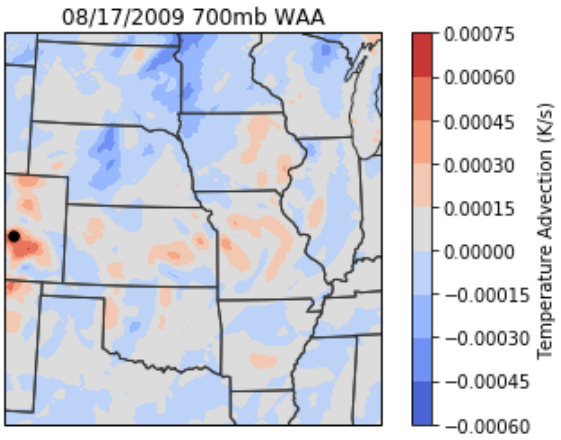

FIG. 2 – Plotting of data on the map of the domain along with the marking of the maximum parameter value in the form of a black dot (700mb Warm Air Advection depicted above).

The differences in both longitude and latitude between the parameter maximum and the centroid of the MCS were analyzed as well. The latitudinal differences ranged from less than a degree to over 8º, with 50% of cases having a latitudinal difference between 2º and 5º (Fig. 4). Longitudinal differences ranged from nearly 0º to approximately 15º, with 50% of cases having a longitudinal difference between 3º and 7º (Fig. 5).

Given the results of the distance and direction analyses, it is apparent that the distance of the maximum point of 700mb WAA to the centroid of an MCS does not provide

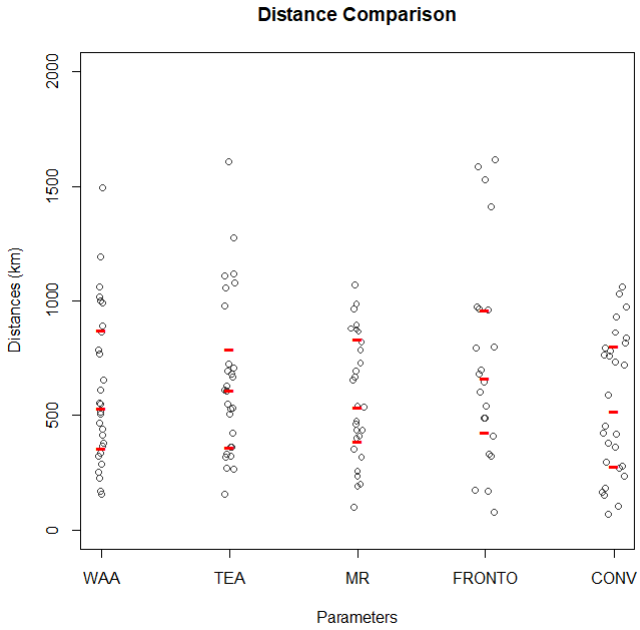

FIG. 3 – Box plots detailing the variation in distances of the five examined parameters: 700mb warm air advection (WAA), 850mb mixing ratio (MR), theta-e advection (TEA), 850mb convergence (CONV), and surface frontogenesis (FRONTO).

consistent results. As can be seen in Figure 3, 75% of cases had a WAA max that was located between 200km and approximately 875km. This is a range of over 600km; a range that would not be particularly useful when trying to forecast an MCS initiation point solely on distance alone. Simply put, there does not appear to be a set distance or a small range of distances which a forecaster could use to determine the initiation point of an MCS. Direction provides more consistent results, given that the max point of WAA was located northeast of the MCS initiation point in 50% of the cases examined. Upon further

analyses of other directions, it was found that cases in which the WAA max was oriented to the west of the MCS initiation point occurred on the front range of the Rocky Mountains. This indicates that downslope adiabatic warming potentially played a role in the calculation of the WAA max, meaning that cases in which this effect occurred do not accurately represent the true direction of the WAA max with respect to the MCS initiation point.

An analysis of WAA latitudinal differences did not yield any meaningful results. One area of slight notice is the condensed cluster of cases where the latitudinal difference was just over two degrees, but otherwise, the range of differences was broad. Analyzing WAA longitudinal differences resulted in similar findings. The lack of any condensed ranges incorporating a large number of cases for both latitudinal and longitudinal differences would suggest that there is little application to forecasting potential regarding these differences.

b. 850mb Mixing Ratio

850mb mixing ratio also displayed a wide range of distances from its maximum point to the centroid of an MCS, albeit not to the extent of other parameters. On average, the maximum point of the mixing ratio was located approximately 580km away from the MCS centroid, with maximum and minimum distances of 1073km and 101km respectively (Fig. 3).

A directional analysis demonstrated a wide range of directions with which the mixing ratio maximum could be found with respect to the MCS centroid. The most consistent direction with which the mixing ratio maximum appeared was to the southwest of the MCS initiation point, occurring in 32% of all cases. Following that, southeast and easterly directions occurred in 18% and 14% of cases respectively. Mixing ratio

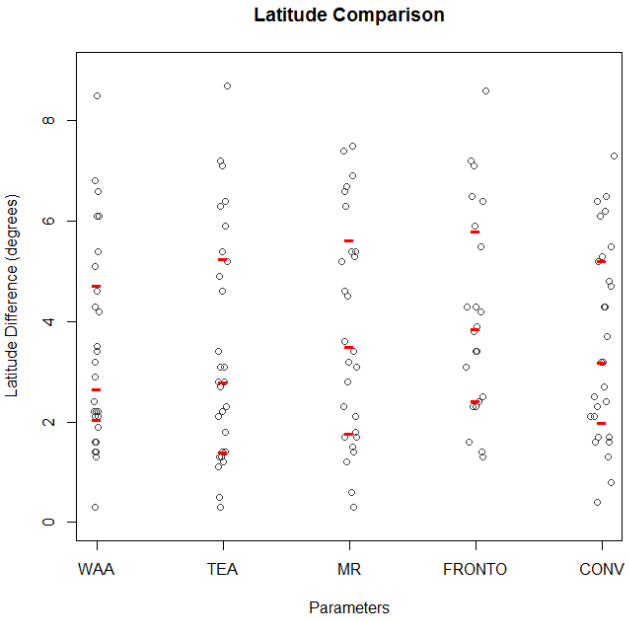

FIG. 4 – Box plots detailing the difference in latitudes of the five examined parameters with respect to the MCS centroid: 700mb warm air advection (WAA), 850mb mixing ratio (MR), theta-e advection (TEA), 850mb convergence (CONV), and surface frontogenesis (FRONTO). This latitudinal difference refers to the difference between the latitude of the parameter maximum and the latitude of the MCS centroid.

maximums were found to the south and northeast in 11% of cases (for both directions), and maximums were also found to the northwest and west in 7% of cases (for both directions).

Similarly to WAA, latitudinal and longitudinal differences between mixing ratio maximums and centroids of MCSs were analyzed. A wide range of latitudinal differences was observed, from a minimum of approximately 0.4º to a maximum of just under 8º (Fig. 4). 50% of cases presented with

a latitudinal difference between two degrees and six degrees. Longitudinal differences ranged from a minimum of approximately 0.3º to a maximum of approximately 13º (Fig. 5). 50% of cases presented with a longitudinal difference between two and five degrees. Generally, longitudinal differences appeared to be clustered between the 0-5º difference ranges.

Although not as broad as some of the other parameters examined and having a marginally lower average distance, 850mb mixing ratio displayed a wide range of distances from its maximum point to the centroid of an MCS. Using similar reasoning from examining WAA results, it also appears that distance does not provide a consistent value or range of values within which an MCS initiates, meaning examining distance would not be particularly useful when

forecasting an MCS initiation point. It also appears that there is no consistent direction

where a mixing ratio maximum exists with respect to an MCS initiation point. At best, only 32% of cases agreed on a direction, which is not as good when comparing it to WAA directions. Additionally concerning is the wide spread of directions where the maximum was located. A total of seven directions were observed in the study when analyzing 850mb mixing ratio, further providing evidence that there is no clearly defined direction where the mixing ratio maximum occurs with respect to the MCS initiation point.

An analysis of the longitude and latitude differences of the 850mb mixing ratio also yields little helpful information. Ranges in both latitude and longitude differences are wide, with there not being a small range of differences (~2-3º) where a 50% of the cases lie (Figs. 4, 5). Given this, it does not appear that longitude and latitude differences are correlated with the initiation

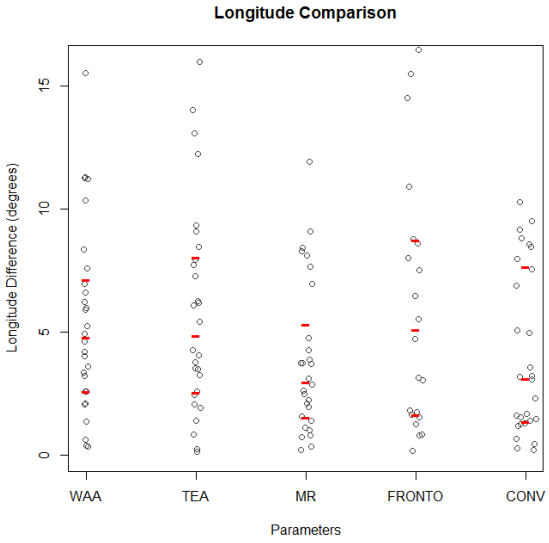

FIG. 5 – Box plots detailing the difference in longitudes of the five examined parameters: 700mb warm air advection (WAA), 850mb mixing ratio (MR), theta-e advection (TEA), 850mb convergence (CONV), and surface frontogenesis (FRONTO). This latitudinal difference refers to the difference between the latitude of the parameter maximum and the latitude of the MCS centroid.

point of an MCS in a meaningful or helpful

forecasting sense. However, it must be mentioned that longitudinal differences in mixing ratio did tend to congregate in the 0-5º range. While broader than the desired 2-3º range, this observation could provide some potential benefit to operational forecasters, knowing that slightly over 50% of cases tend to have a latitudinal difference between the mixing ratio maximum and MCS initiation centroid of the aforementioned observed range.

c. 850mb Equivalent Potential Temperature Advection

850mb Θ_E advection demonstrated the second largest range of distances from the Θ_E advection maximum to the centroid of the

MCS. On average, Θ_E advection maxes were found at a distance of 660km away from the centroid of the MCS on radar composite reflectivity, with maximum and minimum distances of 1606km and 159km respectively. 50% of cases experienced a range of distances from around 380km to 840km (Fig. 3).

Analysis of 850mb Θ_E advection maximum direction from the MCS centroid shows a wide range of directions. Easterly directions tended to be favored, with maximums located in the northeast occurring in 32% of cases, and maximums located in the southeast and east in 21% of cases for both directions. Maximums located in the southwest occurred in 18% of cases, with the final 8% of cases having maximums in the south and west directions (evenly split percentage).

Analyses of the latitudinal and longitudinal differences between the point of maximum Θ_E advection and the centroid of the MCS yielded a wide range of differences. Latitudinal differences were found in a range from approximately 0.3º to 8.5º, with 50% of the cases falling in the difference range between 1.6º and 5.6º (Fig. 4). Longitudinal differences exhibited a very wide range from a minimum of nearly 0º to a maximum of 15.7º, with 50% of cases falling into a difference range between 2.5º and 7.5º (Fig. 5).

As with the previous parameters, an analysis of distances from the 850mb Θ_E advection maximum to the centroid of the MCS yielded little useful information with respect to operational forecasting. Directions, while broad, did demonstrate that Θ_E advection maximums tended to occur in easterly directions (NE, SE, E) in 74% of cases, with the northeasterly direction being favored in 32% of cases. Analysis of latitudinal and longitudinal differences did not yield much useful information. Ranges in both differences were extremely broad, and no noticeable clusters of cases were found at any difference value or a small range of difference values. Overall, distance, latitudinal differences, and longitudinal differences do not appear to be a useful source of information when forecasting the initiation point of an MCS. Direction could be a potentially useful indicator, as the large majority of cases favored eastern directions.

d. Surface Frontogenesis

Analysis of surface frontogenesis distances from the maximum of the parameter to the centroid of the MCS yielded the widest range of distances of all the examined parameters. The parameter averaged a distance of 739km from the maximum to the centroid, with maximum and minimum distances of 1617km and 80km (Fig. 3).

An analysis of surface frontogenesis directions from the parameter maximum to the MCS centroid yielded 7 different directions: north (5% of cases), northeast (32%), east (9%), southeast (5%), south (18%), southwest (27%), and west (4%).

Both latitudinal and longitudinal differences were analyzed for surface frontogenesis. Latitudinal differences between the parameter maximum and the MCS centroid fell into a range from approximately 1.6º to 8.4º, with 50% of cases falling into a latitudinal difference range from 2.2º to 5.9º (Fig. 4). Longitudinal differences between the parameter maximum and the MCS centroid fell into a range from approximately 0.2º to 15.9º, with 50% of cases falling into a longitudinal difference range from 2º to 8º (Fig. 5).

Like the previous parameters, forecasting a general MCS initiation location based on distance does not appear to be a viable option given the results of this study. The distance ranges varied the most out of all the parameters examined, and there was no small range of values in a significant portion of the cases. Analyzing direction yields little useful forecasting advice as well. Seven different directions were observed, with there being no standout direction that was observed in 50% of cases or greater, with the closest direction to that being northeast in 32% of cases. Like previous parameters, latitudinal and longitudinal differences between the surface frontogenesis maximum and the centroid of an MCS yielded little helpful information. No noticeable clusters of cases were observed in a small range of difference values, with the only potentially notable instance occurring in the longitudinal difference of approximately 1.5º.

e. 850mb Convergence

850mb convergence maximums occurred on average a distance of 552km away from the MCS centroid. Maximum and minimum distances were found to be 1064km and 70km respectively (Fig. 3).

An analysis of 850mb convergence directions from the parameter maximum to the MCS centroid yielded seven different directions: north (14% of cases), northeast (14%), east (11%), southwest (43%), west (7%), and northwest (11%).

Analyzing latitudinal differences between the 850mb convergence maximum and the centroid of the MCS yielded a wide range of values, similar to the other analyzed parameters. Latitudinal differences ranged from 0.4º to 7.1º, with 50% of cases falling in a difference range from 2.1º to 5.3º (Fig. 4).

Analyzing longitudinal differences yielded a more condensed range of values that fell between 0.3º and 10.4º, with 50% of cases falling in a difference range between 1.4º and 7.2º (Fig. 5).

Similar to the other parameters, distances of 850mb convergence maximums from an MCS centroid does not appear to be a relevant addition in forecasting initiation points of MCSs. While having the smallest average distance of the parameters, a distance of 552km is not particularly meaningful. Direction yields more useful information, since the convergence maximum was found to the southwest of the MCS initiation point in 42% of cases. Latitudinal differences between the 850mb convergence maximum and the MCS centroid yielded little helpful information, much the same as other parameters. Cases fell into a wide range of differences, with there being no set of cases condensed within a range of a couple degree differences. Longitudinal differences between the 850mb convergence maximum and the MCS centroid yielded slightly more interesting results. Based on Figure 5, it appears that convergence maximums tended to occur approximately 1.7º away from the MCS initiation point.

5. Discussion and Conclusion

Analyzing RUC and RAP data with respect to the five parameters outlined above, this study analyzed the efficacy with which each parameter predicts the initiation location of a warm-season MCS in the Great Plains. Observing overall trends, none of the parameters chosen particularly stood out in terms of its distance from the MCS centroid, its direction from the MCS centroid, latitudinal differences, and longitudinal differences. Some parameters stood out in

certain areas, such as 700mb WAA having its maximum to the northeast in half of the cases, and there is a notable small range of longitudinal differences for a small cluster of the cases analyzed.

Regarding potential forecasting use, distance of parameter maximum from the MCS centroid should not be considered a viable option for any of the aforementioned parameters. The large variations in distance, and the lack of a set of small distances occurring in 50% of cases or greater both point to distance being an unreliable forecasting method. Directions did not tend to yield particularly useful forecasting information, with the exception of two parameters. 700mb WAA maximums were found to the northeast in 50% of cases, and 850mb convergence maximums were found to the southwest in 42% of cases. For these two parameters, it appears that the direction of the parameter maximum may have some operational value. Latitudinal difference variation proved to be unremarkable across all of the examined parameters, as did longitudinal difference variation with one slight exception: 850mb convergence. Convergence maximums tended to occur within an approximately 2º difference range in a small cluster of cases. However, this cluster of cases incorporated only around 25% of the cases analyzed, meaning that this finding may not be particularly significant, especially if one considers a larger sample size where potential flukes are damped out.

These findings are based on a relatively small sample size of 29 cases. One question this raises is how the results would differ over a larger number of MCSs over a greater number of years. Additionally, decreasing the size of the domain could potentially have an impact on the results by eliminating the possibility that the Rocky Mountains contaminate data for some parameters, or that the parameter maximum is in a location unrelated to MCS activity (such as over the Great Lakes as was seen in some cases). More in-depth analyses of these parameters in different study configurations will undoubtedly have to be performed in the future.

Acknowledgements. The author would like to thank Dr. William Gallus, Jr. for his willingness to provide mentorship during the semester. The author would also like to thank Jonathan Thielen for his assistance in programming and data retrieval methods.

REFERENCES

Bluestein, H. B., 1993: *Observations and Theory of Weather Systems. Vol. 2, Synoptic-Dynamic Meteorology in Midlatitudes*. Oxford University Press, 608 pp.

Bolton, D., 1980: The computation of equivalent potential temperature. *Mon. Wea. Rev.*, **108**, 1046-1053, https://doi.org/10.1175/1520-0493(1980)108<1046:TCOEPT>2.0.CO;2

Cotton, W.R., M.S. Lin, R.L. McAnelly, and C.J. Tremback, 1989: A composite model of mesoscale convective complexes. *Mon. Wea. Rev.*, **117**, 765-783, https://doi.org/10.1175/1520-0493(1989)117<0765:ACMOMC>2.0.CO;2

Davies-Jones, R., 2009: On Formulas for Equivalent Potential Temperature. *Mon. Wea. Rev.*, **137**, 3137-3148, https://doi.org/10.1175/2009MWR2774.1

Hobbs, P. V., and J. M. Wallace, 1977: *Atmospheric Science: An Introductory Survey*. Academic Press, 350 pp.

Maddox, R. A., D. J. Perkey, J. M. Fritsch, 1981: Evolution of upper tropospheric features during the development of a mesoscale convective complex. *J. Atmos. Sci.*, **38,** 1664-1674, https://doi.org/10.1175/1520-0469(1981)038<1664:EOUTFD>2.0.CO;2

Maddox, R. A., 1980: Mesoscale convective complexes. *Bull. Amer. Meteor. Soc.*, **61,** 1374-1400, https://doi.org/10.1175/1520-0477(1980)061<1374:MCC>2.0.CO;2

Moore, B. J., P. J. Neiman, F. M. Ralph, F. E. Barthold, 2012: Physical processes associated with heavy flooding rainfall in Nashville, Tennessee, and vicinity during 1-2 May 2010: The role of an atmospheric river and mesoscale convective systems. *Mon. Wea. Rev.*, **140,** 358-378, https://doi.org/10.1175/MWR-D-11-00126.1

Schumacher, R. S., R. H. Johnson, 2005: Organization and Environmental Properties of Extreme-Rain-Producing Mesoscale Convective Systems. *Mon. Wea. Rev.*, **133,** 961-976, https://doi.org/10.1175/MWR2899.1

Squitieri, B. J., W. A. Gallus, 2016: WRF Forecasts of Great Plains Nocturnal Low-Level Jet Driven MCSs. Part I: Correlation between Low-Level Jet Forecast Accuracy and MCS Precipitation Forecast Skill. *Wea. Forecasting*, **31,** 1301-1323, https://doi.org/10.1175/WAF-D-15-0151.1

Squitieri, B. J., W. A. Gallus, 2016: WRF Forecasts of Great Plains Nocturnal Low-Level Jet Driven MCSs. Part II: Differences between Strongly and Weakly Forced Low-Level Jet Environments. *Wea. Forecasting*, **31,** 1491-1510, https://doi.org/10.1175/WAF-D-15-0150.1